Simplified Seismic Response Prediction for Vibration Prone Non-Structural Components in Inelastic Frame Structures

15 WCEE
LISBOA 2012

L. Moschen & C. Adam
Department of Civil Engineering Sciences, University of Innsbruck, Austria

SUMMARY:
A methodology for estimating the seismic peak response of vibration-prone non-structural components (NSCs) is presented. The considered NSCs are modelled as single-degree-of-freedom (SDOF) oscillators, and they are attached to the roof of ductile planar regular frames subjected to earthquake excitation. The methodology is based on floor response spectra of NSCs on SDOF load-bearing structures, and a modified modal superposition procedure. The dynamic interaction between NSCs and the supporting structure is considered, and thus, the seismic response of moderately heavy NSCs can be studied. Seismic excitation is represented by the 44 records of the ATC63 far-field record-set. From the presented results it can be concluded that this methodology is effective to assess sufficiently accurate the peak response of vibration-prone NSCs supported by ductile load-bearing structures.

Keywords: Floor response spectrum; Modal coupling; Modified modal superposition; Non-structural component

1. INTRODUCTION

Strong motion earthquakes of the last decades such as in Northridge (1994), Kobe (1995), and Maule (2010) have demonstrated that the seismic resistance of load-bearing structures is in general sufficient, if they are designed according to actual codes. However, in many cases non-structural building components (NSCs) failed to resist the seismic excitation, which led to huge monetary losses. For example, for a hospital these losses were about 92% of the total construction costs (Taghavi and Miranda 2003). Thus, it is important to consider not only the seismic behaviour of the load-bearing structure, but also to assess the seismic response of NSCs. Since a building may contain numerous NSCs, it is not feasible to conduct a detailed time history analysis for each NSC. Consequently, there is a need for methodologies, which allow an efficient but yet sufficiently accurate prediction of the seismic peak response of NSCs. In particular, if a NSC is moderately heavy and the natural frequencies of the NSC and the supporting structure are closely spaced, the dynamic interaction between the substructures cannot be neglected anymore without considerable overprediction of the NSC peak response. Furthermore, the load-bearing structures are designed to behave inelastically when subjected to severe earthquake excitation. However, inelastic deformations have a grave effect on the dynamic response of NSCs, because the structural behaviour becomes strongly nonlinear, the dynamic peak responses are reduced, and periods are elongated. In such situations, traditional simplified methods of NSC response assessment cannot be used anymore without making large errors.

In the present study a modified modal superposition method is presented, which allows the prediction of the seismic peak response of moderately heavy vibration prone NSCs without major numerical efforts. Thereby, modified floor response spectra of NSCs on SDOF supporting structures are superposed using the SRSS (Chopra 2007) method. The NSCs even may be attached to multi-storey frame structures driven into the inelastic range of deformation in a severe earthquake event. In a previous study (Adam and Furtmüller 2008a) a first mode approximation of the seismic response of NSC on inelastic multi-storey frame structures was examined. However, the authors came to the conclusion that the proposed approximation is inaccurate in the short period range, where higher mode effects become important, in particular when focussing on the acceleration response. In a further study (Adam and Furtmüller 2008b) for unlimited elastic structural assemblies a multi-modal procedure was developed. Here, this procedure is extended to include also the effect of inelastic behaviour of the supporting structure on the NSC response.

2. METHODOLOGY

2.1. Equations of Motion of a Generic Frame Structure Equipped with a Non-structural Element

Regular planar moment resisting single bay frames with N stories and concentrated masses $m/2$ in the corners as shown in Fig. 2.1 represent the supporting structures (Medina and Krawinkler 2003) of this study. In particular, 9-storey ($N = 9$) and 18-storey ($N = 18$) frames are considered. The storey height h is 3.66 m. The frames exhibit a linear first mode shape with a fundamental period of $N/10$ (stiff frames) and $N/5$ (flexible frames), respectively. Bilinear moment resisting springs are located at the ends of the girders and at the base, adding up to a total number of $2(N + 1)$ springs. The hardening ratio of the springs is 0.03. The dynamic degrees-of-freedom (DOFs) of the frame substructures are the horizontal storey displacements with respect to the base w_j, $j = 1, ..., N$. To the Nth floor (roof) an SDOF NSC with lumped mass m_s, stiffness k_s , and damping parameter c_s is attached. The associated DOF is the horizontal displacement x_s (with respect to the base) of the mass m_s.

The $(N + 1)$ equations of motion of the coupled frame-NSC system are formulated separately for each substructure according to (Adam and Furtmüller 2008b)

$$\mathbf{M}\ddot{\mathbf{w}} + \mathbf{C}\dot{\mathbf{w}} + \mathbf{K}\mathbf{w} = -\mathbf{M}\mathbf{1}\ddot{w}_g - \mathbf{G}\boldsymbol{\theta}^{pl} + \mathbf{e}_N\left[k_s\left(x_s - w_N\right) + c_s\left(\dot{x}_s - \dot{w}_N\right)\right] \tag{2.1a}$$

$$\ddot{x}_s + 2\zeta_s\omega_s\dot{x}_s + \omega_s^2 x_s = -\ddot{w}_g + 2\zeta_s\omega_s\dot{w}_N + \omega_s w_N \tag{2.1b}$$

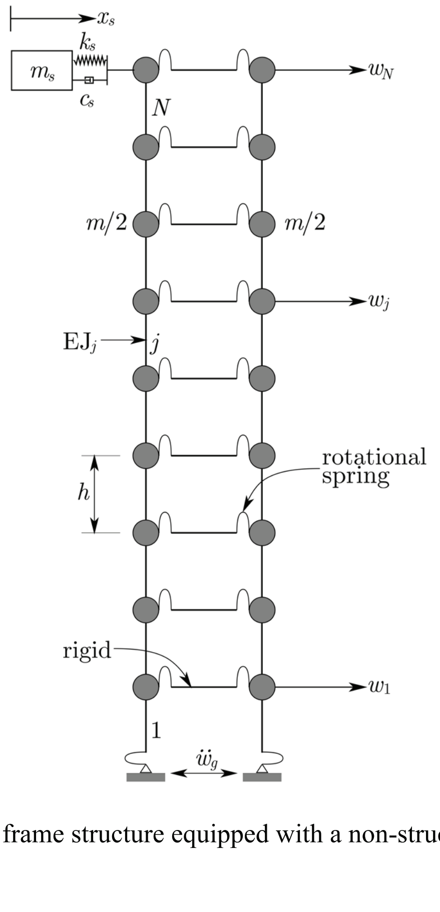

Figure 2.1. 9-storey generic frame structure equipped with a non-structural component at the roof

In these equations the coupling terms between the supporting structure and the NSC are written on the right-hand-side. In Eqns. 2.1a **M**, **C**, and **K** are the mass matrix, proportional damping matrix, and the stiffness matrix, respectively, of the stand-alone frame structure. The modal damping coefficients of the load-bearing structures are $\zeta_j = 5\%$, $j = 1,\ldots, N$. Vector **1** represents the lateral displacements of the lumped masses of this substructure as a consequence of a static unit base displacement in direction of the seismic excitation. **G** is the condensed plastic influence matrix of dimension [N $\times$ 2 (N + 1)], and $\boldsymbol{\theta}^{pl}$ denotes the vector of the plastic rotations in the rotational springs. In the inelastic case the considered frame structures have a target ductility of $\mu = 4$. $\mathbf{e}_N$ describes the dynamic interaction between the frame substructure and the NSC, with the Nth element equal to one, and all other elements equal to zero. Eqn. 2.1b represents the equation of motion of the attached NSC, where ω_s denotes the circular frequency and ζ_s the viscous damping ratio of the decoupled NSC,

$$\omega_s = \sqrt{k_s / m_s}, \quad \zeta_s = c_s / \left(2 m_s \omega_s\right) \tag{2.2}$$

Throughout the study ζ_s is selected to be 1%.

2.2. Modal Representation of the Equations of Motion

Vector $\mathbf{w}$, which represents the storey displacements of the frame structure, is expanded into a modal series (Chopra 2007),

$$\mathbf{w} = \sum_{j=1}^{N} \boldsymbol{\phi}_j q_j \tag{2.3}$$

$\boldsymbol{\phi}_j, j = 1,\ldots,N$, are the N mode shapes of the decoupled supporting structure (without NSC). However, this expansion leaves the equations for the modal coordinates $q_j, j = 1,\ldots,N$, coupled, because the mode shapes are not orthogonal to the mass matrix, the damping matrix, and the stiffness matrix of the complete coupled frame-NSC system. For modal mass ratios

$$\bar{m}_j = \frac{m_s}{\boldsymbol{\phi}_j^T \mathbf{M} \boldsymbol{\phi}_j}, \quad j = 1,\ldots,N \tag{2.4}$$

much smaller than one, $\bar{m}_j \ll 1$, the off-diagonal components of modal equations of motion become small, if the (decoupled) natural frequency of the NSC and (decoupled) natural frequencies of the frame are well separated, and thus may be neglected (Adam and Fotiu 2000). However, if the jth natural frequency ω_j of the frame becomes closely spaced to the natural frequency ω_s of the NSC, coupling between the jth modal frame equation of motion and the equation of motion for the NSC must be considered according to

$$\begin{aligned}
&\begin{bmatrix} 1 & 0 \\ 0 & \bar{m}_j \end{bmatrix} \begin{Bmatrix} \ddot{q}_j \\ \ddot{x} \end{Bmatrix} + \begin{bmatrix} 2\zeta_j \omega_j + 2\zeta_s \omega_s \phi_{j,N}^2 \bar{m}_j & -2\zeta_s \omega_s \phi_{j,N} \bar{m}_j \\ -2\zeta_s \omega_s \phi_{j,N} \bar{m}_j & 2\zeta_s \omega_s \bar{m}_j \end{bmatrix} \begin{Bmatrix} \dot{q}_j \\ \dot{x} \end{Bmatrix} \\
&+ \begin{bmatrix} \omega_j^2 + \omega_s^2 \phi_{j,N}^2 \bar{m}_j & -\omega_s^2 \phi_{j,N} \bar{m}_j \\ -\omega_s^2 \phi_{j,N} \bar{m}_j & \omega_s^2 \bar{m}_j \end{bmatrix} \begin{Bmatrix} q_j \\ x \end{Bmatrix} = -\begin{Bmatrix} \Gamma_j \\ \bar{m}_j \end{Bmatrix} \ddot{w}_g + \begin{Bmatrix} \omega_j^2 \\ 0 \end{Bmatrix} q_j^{pl}
\end{aligned} \tag{2.5}$$

where

$$m_j^* = \boldsymbol{\phi}_j^T \mathbf{M} \boldsymbol{\phi}_j, \quad k_j^* = \boldsymbol{\phi}_j^T \mathbf{K} \boldsymbol{\phi}_j, \quad \omega_j = \sqrt{k_j^* / m_j^*}, \quad \Gamma_j = \boldsymbol{\phi}_j^T \mathbf{M} \mathbf{1} / m_j^* \tag{2.6}$$

The last term in Eqns. 2.5 takes into account the effect of plastic spring rotations:

$$q_j^{pl} = 1/\omega_j^2 \left(\boldsymbol{\phi}_j^T \mathbf{G} / m_j^* \right) \boldsymbol{\theta}^{pl} \tag{2.7}$$

If the mode shapes $\boldsymbol{\phi}_j$ are normalized to leave their Nth element (at the roof level) equal to one, $\phi_{j,N} = 1,\ j = 1,..,N$, the differential operator of Eqns. 2.5 is identical to the one of the equations of motion of a two-degree-of-freedom (2DOF) oscillator, which is composed of two SDOF oscillators connected in series. However, the excitation on the right hand side of Eqns. 2.5 is different. While in the upper equation of Eqns. 2.5 the base excitation is multiplied by the participation factor Γ_j, for a real 2DOF oscillator this factor is equal to one (compare with Adam and Furtmüller 2008c). Thus, floor response spectra based on the equations of motion of a real 2DOF system cannot be used without modification for the solution of Eqns. 2.5. The proposed modification is discussed subsequently.

Note that in this study $\phi_{j,N} = 1,\ j = 1,..,N$, and thus, the modal mass ratios $\bar{m}_j$ and the effective modal ratios $\bar{\bar{m}}_j$, which control the effect of the NSC on the frame structure, coincide,

$$\bar{\bar{m}}_j = \frac{m_s \phi_{j,N}^2}{\boldsymbol{\phi}_j^T \mathbf{M} \boldsymbol{\phi}_j} \equiv \frac{m_s}{\boldsymbol{\phi}_j^T \mathbf{M} \boldsymbol{\phi}_j} = \bar{m}_j, \quad \phi_{j,N} = 1,\ j = 1,..,N \tag{2.8}$$

The effective modal mass ratio $\bar{\bar{m}}_1$ is 5% throughout the study.

2.3. Modified Modal Peak Response Superposition

Since the modal Eqns. 2.5 are similar to the equations of motion of a "real" 2DOF oscillator Adam and Furtmüller (2008b) propose to superpose modally floor response spectra of SDOF NSCs attached to SDOF supporting structures. In the jth utilized 2DOF floor response spectrum denoted as S_j the underlying period T_p, and the damping coefficient ζ_p of the SDOF supporting structure, respectively, are to be equal to the jth period T_j, and the jth modal damping coefficient ζ_j of the jth mode of the actual supporting structure with the same target ductility μ: $T_p = T_j,\ \zeta_p = \zeta_j$. Furthermore, the properties of the NSC of 2DOF floor response spectrum and of the considered counterpart must be identical. Note that 2DOF floor response spectra may be determined in advance and might be available in a database in the future. 2DOF floor response spectra must be modified, because the excitation of the modal equations is different compared to a 2DOF system. That is, they are multiplied by an effective participation factor $\bar{\Gamma}_j$ (Adam and Furtmüller 2008b) before they can be superposed according to the SRSS method,

$$\bar{S} = \sqrt{\sum_{j=1}^{n} \left(\bar{\Gamma}_j S_j \right)^2} \tag{2.9}$$

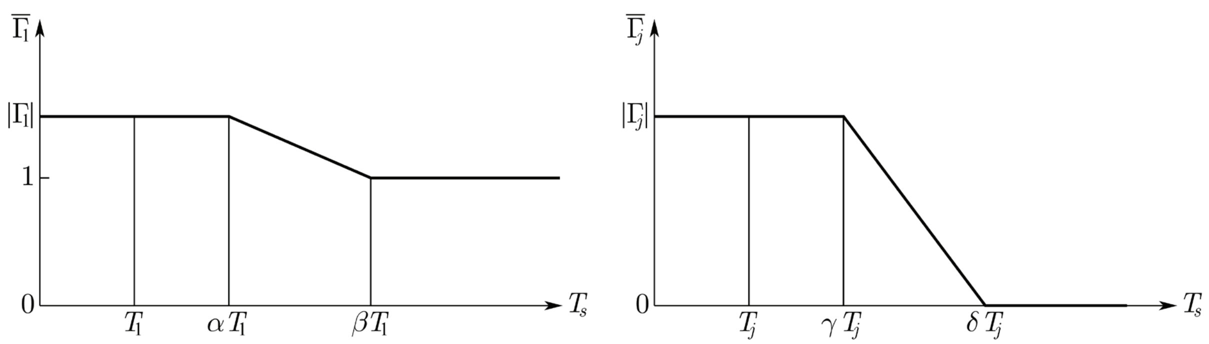

Figure 2.2. Gamma-functions (a) for the first mode, and (b) for higher modes

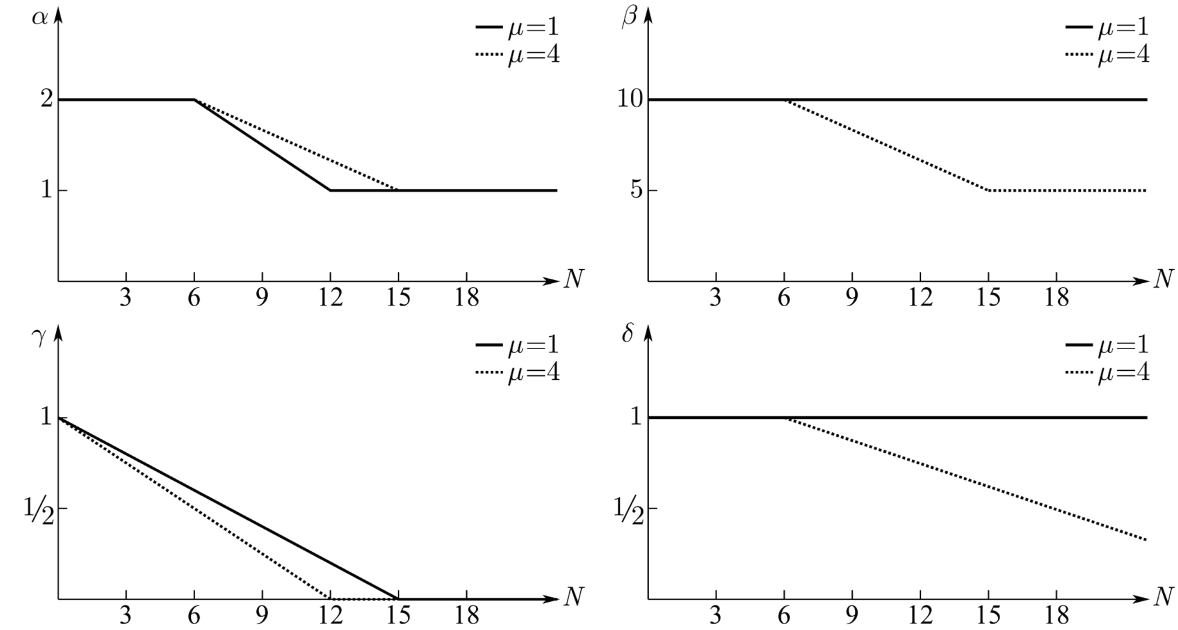

Figure 2.3. Parameters α, β, γ and δ for stiff frames

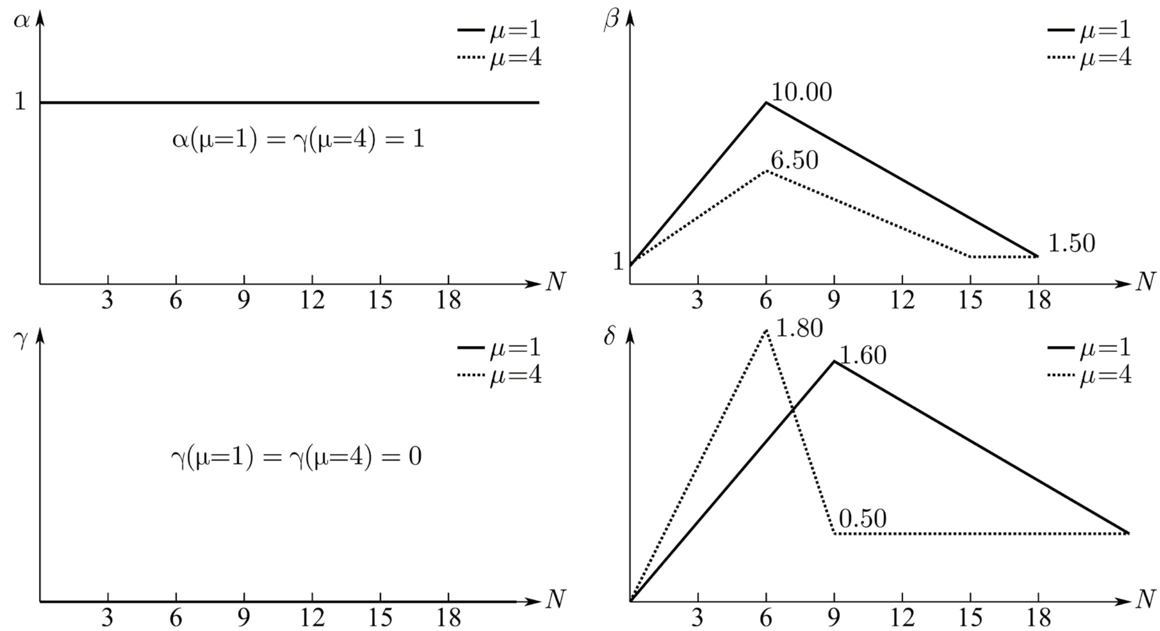

Figure 2.4. Parameters α, β, γ and δ for flexible frames

Thereby, it is assumed that the estimate $\overline{S}$ approximates sufficiently accurate the actual floor response spectrum S of the NSC on the MDOF supporting structure. In Eqn. 2.9 n is the number of considered modes, $n \leq N$. As outlined in Moschen (2010), the effective participation factor $\overline{\Gamma}_j$ depends on the period of the NSC and on the target ductility of the supporting structure. Subsequently, the effective participation factors are referred to as gamma-functions. As shown in Fig. 2.2, where the gamma-functions are plotted against the NSC period $T_s(=2\pi/\omega_s)$, the shape of these functions is different for the first mode and for the higher modes. For short period (almost rigid) NSCs, $T_s < T_j$ ($T_j = 2\pi/\omega_j$), the peak response of the NSC is approximately the same as the modal storey response, where the NSC is attached. Thus, in this period range the gamma-function $\overline{\Gamma}_j$ corresponds to the absolute value of the (original) participation factor $\left|\Gamma_j\right|$, see Eqn. 2.6. For long period NSCs, $T_s > T_j$, the NSC is flexible compared to the supporting structure, and thus, the influence of the supporting structure on the NSC peak response is negligible, and depends mainly on the ground acceleration $\ddot{w}_g$. Thus, for the fundamental mode the gamma-function is 1, and 0 for higher modes. If the substructure periods become tuned, $T_s \approx T_j$, interaction between the supporting structure and the NSC is important, and it is reasonable that for tuned periods the gamma-function corresponds to the original participation factor. Based on numerous example problems and a nonlinear optimization procedure Moschen (2010) determined coefficients α, β, γ and δ, which define the sections of the gamma-functions. In Figs. 2.3 and 2.4 these coefficients are shown for stiff and flexible frames, respectively, as a function of the storey number N and the target ductility μ.

2.4. Seismic Response of Generic Frames with Predefined Target Ductility

In this study for a predefined global target ductility of the supporting frame structure,

$$\mu = \max\left|w_N\right| / w_{N,y} \tag{2.10}$$

the peak response of NSCs is assessed. $w_{N,y}$ is the roof displacement at the onset of yield. The seismic structural response for a predefined target ductility needs to be determined iteratively, and thus, the response prediction becomes very time consuming for systems with many dynamic DOFs. To reduce the numerical efforts, in the presented example problems the appropriate yield strength of the moment resisting springs for a particular predefined target ductility is estimated based on an equivalent SDOF (ESDOF) system of the generic frame structure (Fajfar 2002). Thereby, the shape vector of the ESDOF system corresponds to the first mode of the actual MDOF frame. The outcome of the iterative process involving the considered earthquake record is the strength f_y of the ESDOF system. The base shear at yield V_y of the actual frame structure is related to f_y by

$$V_y = \Gamma_1 f_y \tag{2.11}$$

Subsequently, from V_y the yield strengths of the individual springs are determined.

3. APPLICATION

In several examples it is tested, whether the proposed modified modal superposition of 2DOF floor response spectra leads to reliable estimates of floor response spectra for simple vibration prone NSCs attached to regular multi-storey moment resisting frame structures.

3.1. Ground Motions of the ATC63 Far-Field Record Set

The proposed methodology is tested using a set of ground motions recorded during various seismic events. This set contains 22 records selected from the PEER NGA database with two components of each record, i.e. altogether 44 records. Eight earthquake events in California and six in other countries all over the world are the basis for this earthquake set. The earthquake magnitudes range from 6.5 to 7.6, and the site to source distances are between 11.1 and 26.4 km. The sites of 16 recorded ground motions are classified as site class D (stiff soil sites). The remaining sites are categorized into class C (very stiff soils). Detailed information can be obtained from FEMA (2009).

3.2. Floor Response Spectra

In a first example NSCs attached to the roof of a stiff 9-storey frame structure with a fundamental period of $T_1 = 0.9\,s$ and a target ductility μ of 4 are considered. The presented results are based on the median of each individual seismic response to one record of the ATC 63 earthquake record set. In particular, the seismic median peak response of NSCs with periods ranging from T_s = 0.025 s up to

5 s is assessed, that is the median maximum stroke ΔS_{ds} and the median absolute peak component acceleration S_{as},

$$\Delta S_{ds} = \text{median}\left(\max\left|x_s - w_N\right|\right) \quad , \quad S_{as} = \text{median}\left(\left|\ddot{x}_g + \ddot{x}_s\right|\right) \tag{3.1}$$

In Fig. 3.1 these quantities are plotted against the NSC period T_s. The bold black line corresponds to the outcomes from an analysis involving the full set of coupled equations of motion Eqns. 2.1. Furthermore, the first five modal peak response quantities, which are based on modified 2DOF floor response spectra,

$$\begin{aligned} \Delta\bar{S}_{ds,j}(T_s,\zeta_s,T_p,\zeta_p) &= \text{median}\left(\max\left|x_s(T_s,\zeta_s) - x_p(T_p = T_j,\zeta_p = \zeta_j)\right|\right)\bar{\Gamma}_j \\ \bar{S}_{as,j}(T_s,\zeta_s,T_p,\zeta_p) &= \text{median}\left(\left|\ddot{x}_{s,abs}(T_s,\zeta_s,T_p = T_j,\zeta_p = \zeta_j)\right|\right)\bar{\Gamma}_j \end{aligned} \tag{3.2}$$

are depicted. It is readily seen that the peak stroke ΔS_{ds} is sufficiently accurate approximated by the contribution $\Delta\bar{S}_{ds,1}$ of the first mode only. In contrast, for the peak acceleration response S_{as} in the period range $T_s < T_1$ the superposition of at least three modes according to the SRSS method is necessary for this particular structural assembly. However, the fundamental mode approximates S_{as} in period ranges $T_s \geq T_1$ very well. Thus, the assumption that in the period range $T_s > T_j$ the effective participation factor $\bar{\Gamma}_j$ is zero for higher modes ($j > 1$) is reasonable (see also Fig. 2.2b).

3.2.1. Stroke

Fig. 3.2 shows median floor response spectra for the stroke of NSCs attached to both elastic and inelastic stiff 9-storey frame structures. The black line is the "exact" outcome of a fully coupled computation of the NSC stroke, whereas the red line is the proposed approximation based on the modal superposition of modified 2DOF floor response spectra, Eqn. 3.2,

$$\Delta\bar{S}_{ds} = \sqrt{\sum_{j=1}^{3}\left(\Delta\bar{S}_{ds,j}\right)^2} \tag{3.3}$$

The blue line illustrates the decoupled solution neglecting the interaction between both substructures. In the corresponding analysis the time history of the total roof acceleration serves as excitation of the NSC. The results of Fig. 3.2 show that for a modal mass ratio of 5% a decoupled consideration overestimates the peak stroke considerably, if the fundamental period of the frame and the period of the NSC are closely spaced. This holds true for elastic as well as inelastic structural behaviour.

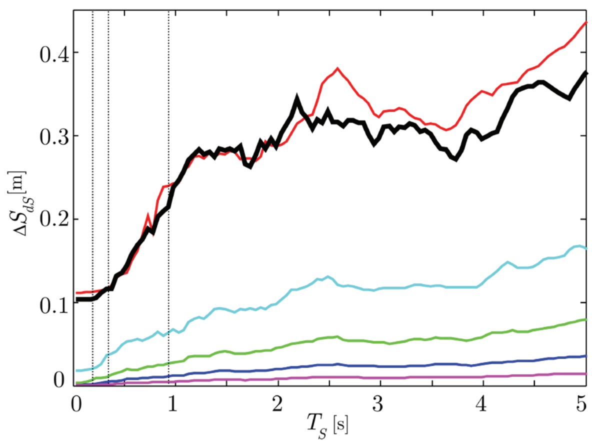

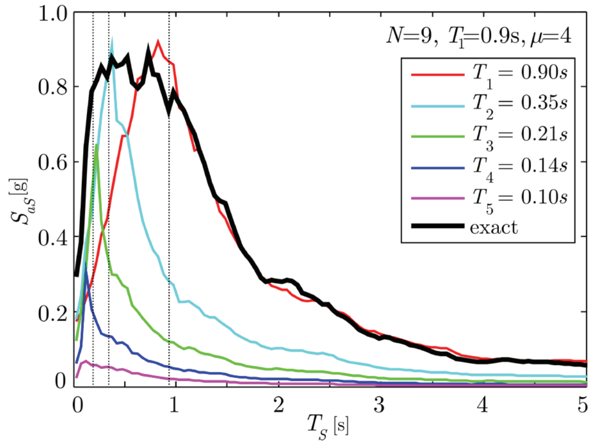

Figure 3.1. Floor response spectra and modal contributions based on 2DOF floor response spectra. Stiff 9-storey supporting structure. Target ductility $\mu = 4$. (a) Median stroke ΔS_{ds}. (b) Median absolute peak acceleration S_{as}

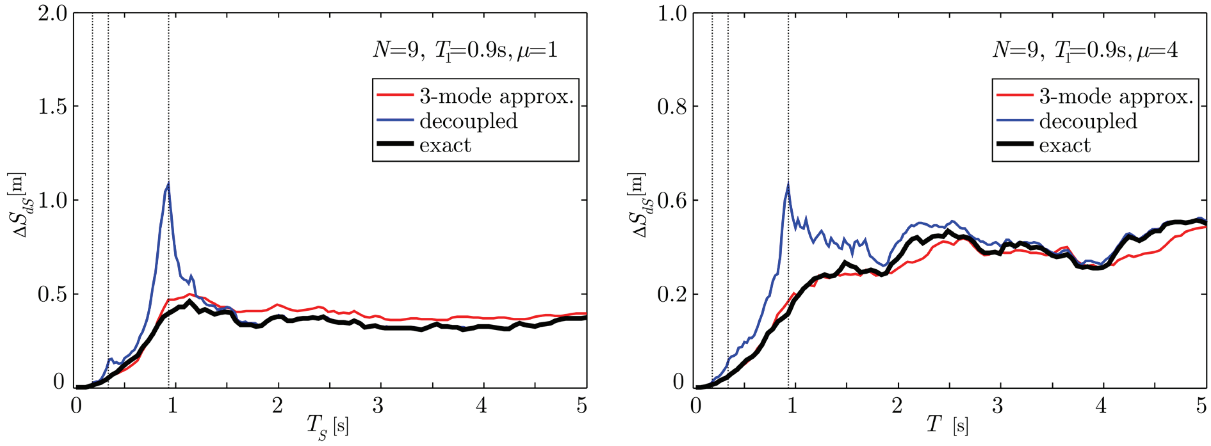

Figure 3.2. Floor response spectra for the median peak stroke ΔS_{ds}. Stiff 9-storey supporting structure. (a) Elastic structure. (b) Inelastic structure with target ductility $\mu = 4$

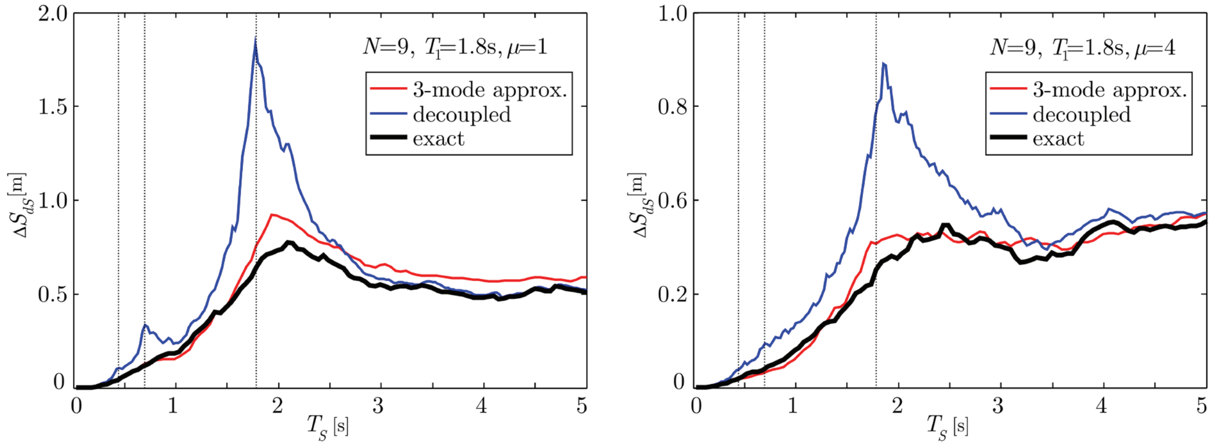

Figure 3.3. Floor response spectra for the median peak stroke ΔS_{ds}. Flexible 9-storey supporting structure. (a) Elastic structure. (b) Inelastic structure with target ductility $\mu = 4$

In Fig. 3.3 floor response spectra for NSCs attached to a flexible 9-storey frame structure with a fundamental period of $T_1 = 1.8\,s$ are depicted. In essence, the same conclusions can be drawn as for the stiff 9-storey structures.

3.2.2. Absolute peak component acceleration

Figs. 3.4 and 3.5 show corresponding floor response spectra for the peak component acceleration. Again, "exact" outcomes from fully coupled simulations (black lines), approximations based on the modal superposition of three modified 2DOF response spectra (red lines), and decoupled acceleration responses (blue lines) are depicted. It can be readily seen that for the more flexible structure the peak acceleration is at maximum, if the NSC period is tuned to the second period T_2 of the frame structure. For this structure even the third mode considerably affects the NSC acceleration response. Compared to the decoupled outcome the proposed simplified methodology predicts quite accurately the absolute peak acceleration for tuned frequencies in the entire range of NSC periods.

In a further example a stiff and a flexible 18-storey frame, both elastic ($\mu = 1$) and inelastic ($\mu = 4$), respectively, support SDOF NSCs with periods T_s ranging from 0.025 s to 5 s. The corresponding acceleration floor response spectra are shown in Figs. 3.6 and 3.7. The proposed approximation overestimates almost in the entire spectral range slightly the peak acceleration of the NSCs, see Fig. 3.6b. However, also these outcomes indicate that the proposed modal superposition procedure may be an appropriate tool for predicting floor response spectra.

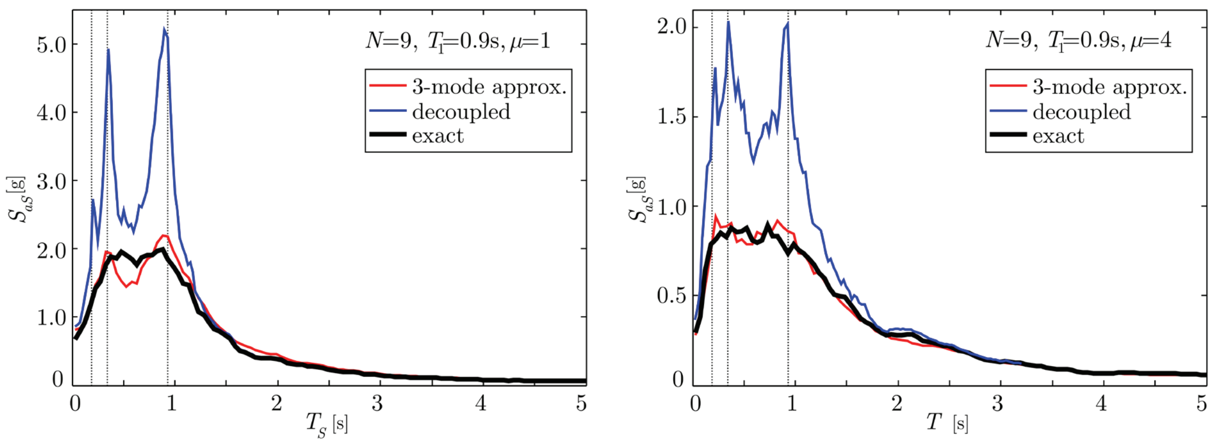

Figure 3.4. Floor response spectra for the median absolute peak component acceleration S_{as}. Stiff 9-story supporting structure. (a) Elastic structure. (b) Inelastic structure with target ductility $\mu = 4$

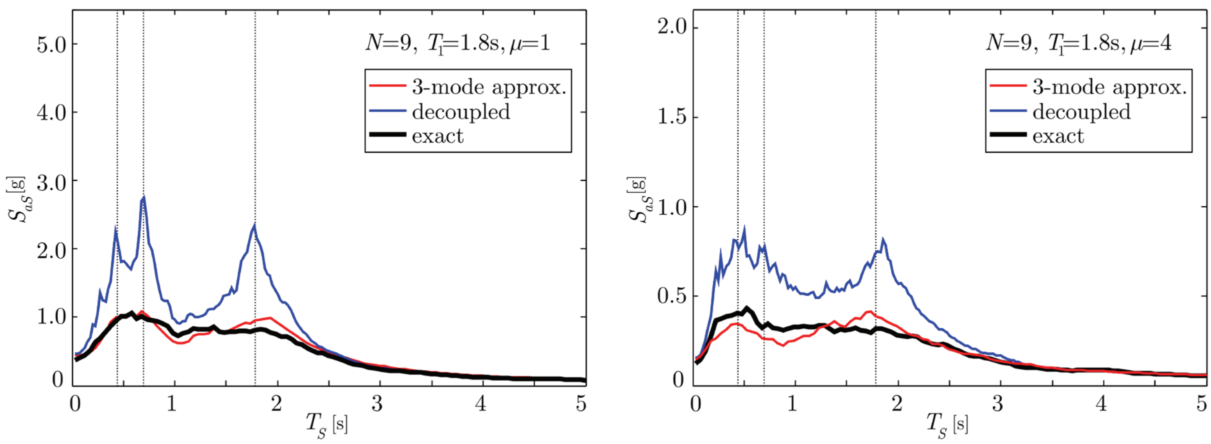

Figure 3.5. Floor response spectra for the median absolute peak component acceleration S_{as}. Flexible 9-storey supporting structure. (a) Elastic structure. (b) Inelastic structure with target ductility $\mu = 4$

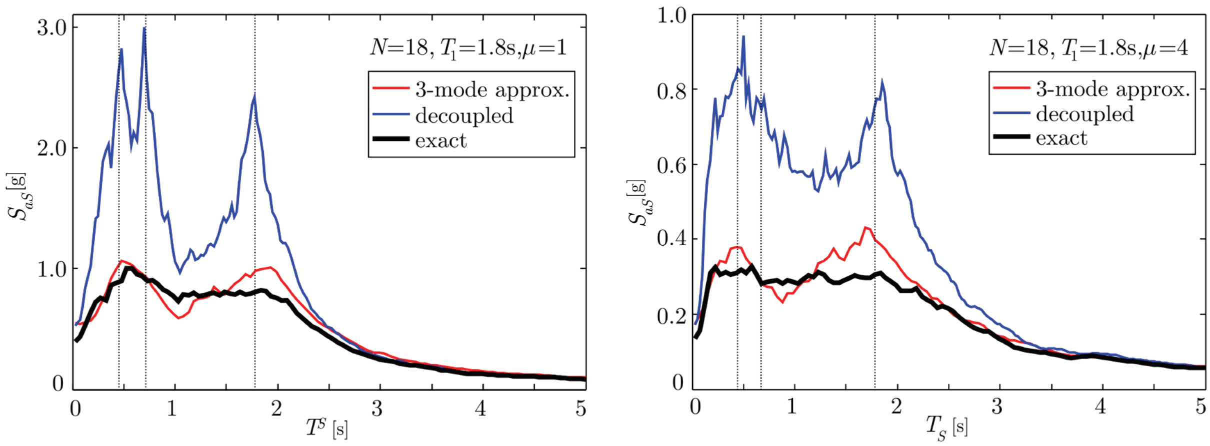

Figure 3.6. Floor response spectra for the median absolute peak component acceleration S_{as}. Stiff 18-storey supporting structure. (a) Elastic structure. (b) Inelastic structure with target ductility $\mu = 4$

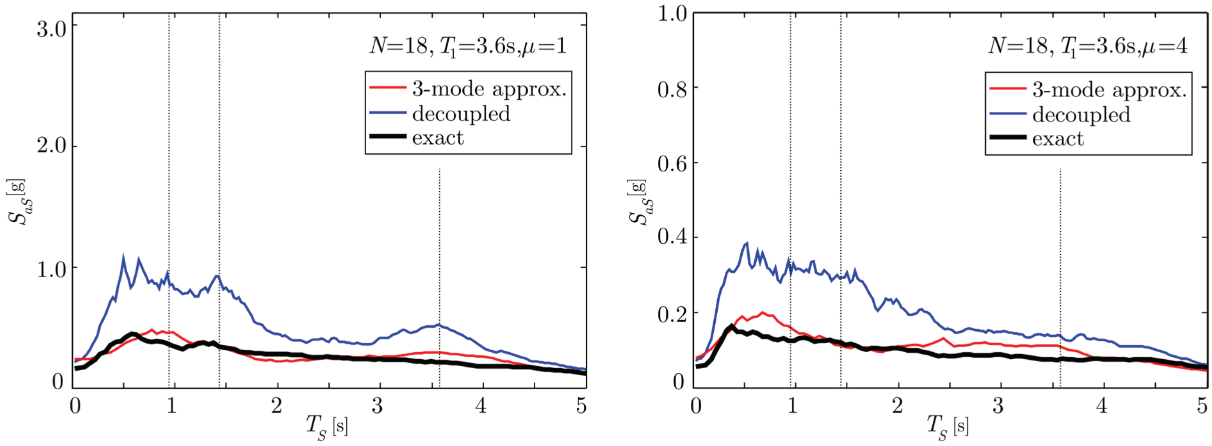

Figure 3.7. Floor response spectra for the median absolute peak component acceleration S_{as}. Flexible 18-storey supporting structure. (a) Elastic structure. (b) Inelastic structure with target ductility $\mu = 4$

4. CONCLUSIONS

The results of this study show that floor response spectra based on a two-degree-of-freedom assembly of a non-structural component (NSC) and a supporting structure can be utilized to predict a floor response spectrum of a NSC on a multi-storey frame structure. However, these floor response spectra must be modified as suggested before they can be modally superposed. The proposed methodology can be applied both for elastic and inelastic behaviour of the supporting structure.

REFERENCES

Adam, C. and Fotiu, P.A. (2000). Dynamic analysis of inelastic primary-secondary systems. *Engineering Structures* **22**, 58-71.

Adam, C. and Furtmüller, T. (2008a). Response of nonstructural components in ductile load-bearing structures subjected to ordinary ground motions. *Proc. of the 14th World Conference on Earthquake Engineering* (14 *WCEE*), October 12 - 17, 2008, Beijing, China, CD-ROM paper, paper no. 05-01-0327, 8pp.

Adam, C. and Furtmüller, T. (2008b). Approximation of the Seismic Response of Vibration Prone Nonstructural Elements Attached to Multi-Story Frame Structures. *Proc. of the Eleventh East Asia-Pacific Conference on Structural Engineering & Construction* (*EASEC*-11), November 19 - 21, 2008, Taipei, Taiwan (Yang, Y.B. et al., eds), CD-ROM paper, paper no. B07-22, 10pp.

Adam, C. and Furtmüller, T. (2008c). Seismic response characteristics of nonstructural elements attached to inelastic buildings. *Structural Dynamics-EURODYN2008, Proc. of 7th European Conference on Structural Dynamics*, July 7 - 9, 2008, University of Southampton, Southampton, UK (Brennan, M.J., ed.), CD-ROM paper, paper no. 120, 12pp.

Chopra, A.K. (2007). Dynamics of structures. Pearson Prentice Hall, Upper Saddle River, N.J.

Fajfar, P. (2002). Structural analysis in earthquake engineering – A breakthrough of simplified non-linear methods. *Proceeding of the 12th European Conference on Earthquake Engineering*.

FEMA (2009). Quantification of building seismic performance factors, *FEMA P695*.

Medina, R.A. and Krawinkler, H. (2003). Seismic demands for nondeteriorating frame structures and their dependence on ground motions. *Report No. 144. The John A. Blume Earthquake Engineering Center, Stanford University.*

Moschen, L. (2010). Abschätzung der Erdbebenantwort schwingungsfähiger Sekundärstrukturen in ebenen Rahmentragwerken. Diploma thesis, University of Innsbruck (in German).

Thagavi, S. and Miranda, E. (2003). Response assessment of nonstructural building elements. *PEER Report 2003/05*. Pacific Earthquake Engineering Research Center, Berkeley CA.